Electronic Supplementary Material (ESI) for Faraday Discussions.

Towards the systematic crystallisation of molecular ionic cocrystals: insights from computed crystal form landscapes

Sharmarke Mohamed,[*a] Ahmad. A. Alwan,[a] Tomislav Friščić,[b] Andrew J. Morris[c] and Mihails Arhangelskis[b]

[a] Department of Chemistry, Khalifa University of Science and Technology, PO Box 127788, Abu Dhabi, United Arab Emirates.

[b] Department of Chemistry, McGill University, 801 Sherbrooke St. W., H3A 0B8 Montreal, Canada.

[c] School of Metallurgy and Materials, University of Birmingham, Edgbaston, Birmingham B15 2TT, UK.

[*]Corresponding author. E-mail: sharmarke.mohamed@kustar.ac.ae

1.1 Conformations for the 4-hydroxybenzoate anion assumed in predicting the crystal structures for Systems II and V

1.1.1 Methodology

The calculated [MP2/6-31G(d,p)] gas phase conformational energy minimum of the 4-hydroxybenzoate anion adopts a planar conformation with a torsion angle of 0 ° for the C3-C2-C1-O2 dihedral (intramolecular degree of freedom for this dihedral angle is shown in the inset to Figure S1 below). By contrast, the conformation of this ion found in the experimental structure of System **V** (**SOLGUX**[1]) is non-planar with a value of -27 ° for the same torsion angle. It has previously been reported[2] that for flexible molecules, favourable intermolecular interactions in the crystal can lead to distortions in the calculated global minimum conformation by up to 20 kJ mol^{-1}. A relaxed dihedral angle scan was performed [MP2/6-31G(d,p); using GAUSSIAN09[3]] for conformations adopted by the 4-hydroxybenzoate ion starting with the gas phase conformational energy minimum. The C3-C2-C1-O2 dihedral angle was scanned in 72 steps with increments of 5 ° per step. For System **V**, a constrained gas phase optimisation of the 4-hydroxybenzoate anion was also performed using as a starting point, the experimental conformation of the anion extracted from the **SOLGUX** crystal structure and optimising all intramolecular degrees of freedom except the C3-C2-C1-O2 dihedral angle. The resulting conformation was also used in the polymorph predictions for System **V** and is denoted as “Conf0” (see Table S7). For Systems **II** and **V**, the labels for the input molecular conformations for the 4-hydroxybenzoate anion as well as the relative energies of these conformations with respect to the gas phase global minimum conformation (denoted *GM*) are listed in Table S1. Figure S1 below shows the potential energy surface for the relaxed scan about the C3-C2-C1-O2 torsion angle.

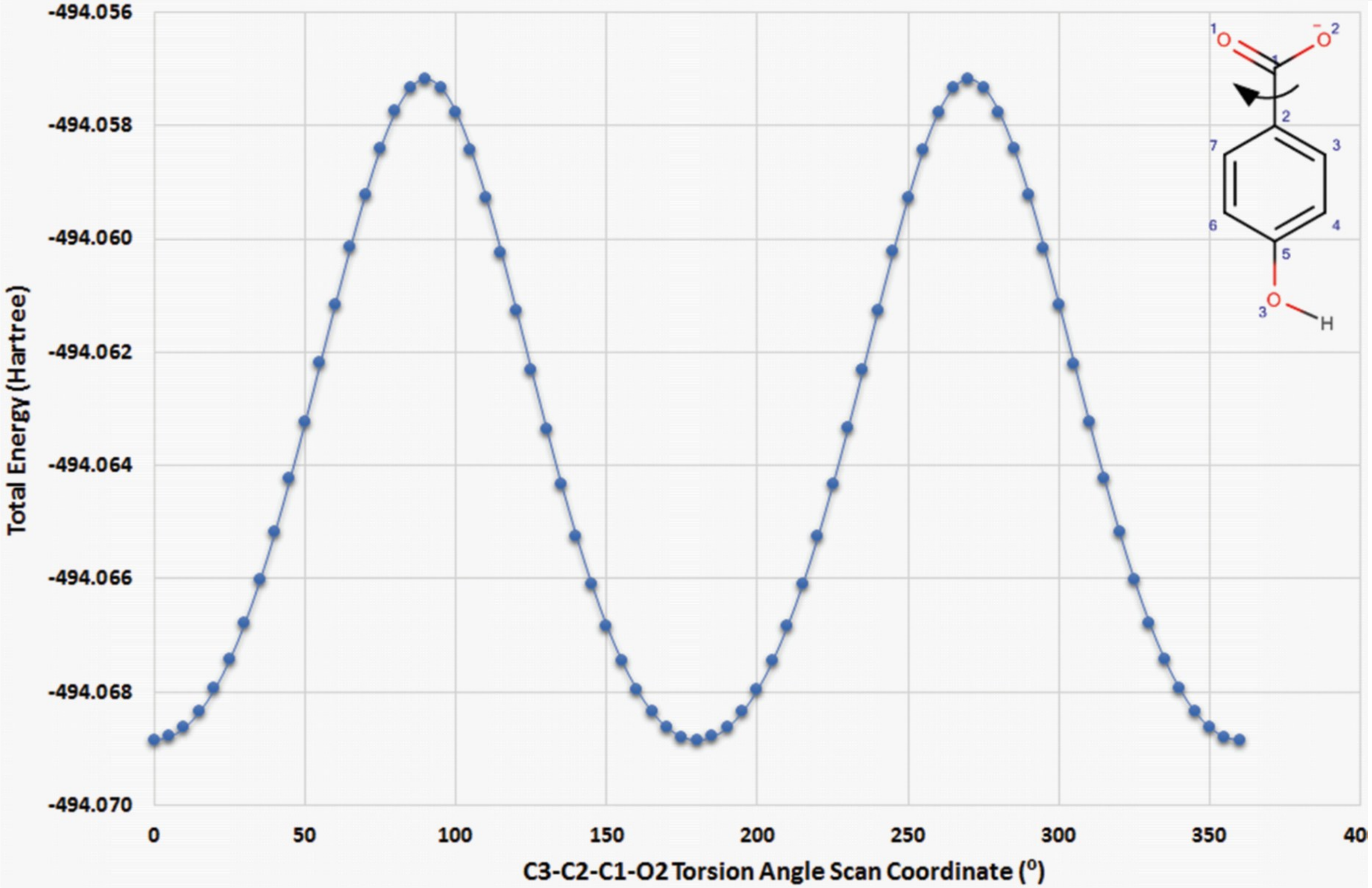

Figure S1: Potential energy surface (PES) for the relaxed scan of the C3-C2-C1-O2 torsion angle of the 4-hydroxybenzoate anion as derived using GAUSSIAN09[3]. The input geometry for the scan was the gas phase conformational energy minimum of the 4-hydroxybenzoate anion. A total of 72 steps were taken during the scan in increments of 5 ° per step. The inset on the top right hand corner shows the molecular structure of the 4-hydroxybenzoate anion with the numbering system used in the calculations. The arrow symbolises the dihedral angle that was scanned.

Conformer Identifier	C3-C2-C1-O2 Torsion Scan Angle (°)	Relative Conformational Energy (ΔE_{intra})
GM	0	0.00
Conf1	165	1.30
Conf2	160	2.33
Conf3	155	3.66
Conf4	150	5.29
Conf5	145	7.22
Conf6	140	9.40
Conf7	195	1.31
Conf8	200	2.34
Conf9	205	3.67
Conf10	210	5.31
Conf11	215	7.23
Conf12	220	9.42

Table S1: Calculated input conformations for the 4-hydroxybenzoate anion used in the rigid body crystal structure prediction for polymorphs of Systems **II** and **V**. The calculated gas phase global minimum energy conformation is denoted *GM*. All other conformations were derived by performing a relaxed scan using GAUSSIAN09[3] by sampling rotations about the C3-C2-C1-O2 dihedral angle according to the methodology outlined in Section 1.1.1 above.

1.2 Calculated molecular properties of acid-base pairs with known ICC crystal structures

	Acid and Base Molecular Properties													
	Molecular Wt. (amu)		CPK Area (Å²)		CPK Volume (Å³)		PSA (Å²)		CPK Ovality		HBD Count		HBA Count	
CSD Refcode for ICC Structure	Acid	Base	Acid	Base	Acid	Base	Acid	Base	Acid	Base	Acid	Base	Acid	Base
AFORIY	212.117	194.237	192.45	205.1	166.89	198.17	108.889	26.512	1.31	1.25	1	1	7	2
AJEBIA	228.116	79.102	199.26	105.39	173.94	89.51	124.026	6.844	1.32	1.09	2	0	8	1
AYUSIX	167.12	121.183	166.59	162.34	144.56	141.92	71.39	6.56	1.25	1.23	1	0	4	1
CAYJAO01	212.117	79.102	192.38	105.74	166.23	89.68	108.899	6.615	1.32	1.09	1	0	7	1
CUKNON	156.568	122.171	157.22	154.98	137.4	137.26	32.66	7.713	1.22	1.2	1	0	1	2
CUKNUT	138.122	122.171	150.78	154.19	130.99	136.68	52.406	7.702	1.21	1.2	2	0	2	2
DIQJEU	254.15	250.345	229.96	268.84	206.05	264.01	130.952	13.049	1.36	1.35	4	0	4	2
DUPJEE	122.123	109.132	141.11	129.17	123.37	108.93	33.225	49.959	1.18	1.17	1	2	1	3
FIJDUX	226.144	138.194	209.66	148.54	184.74	128.84	109.146	27.308	1.34	1.2	1	1	7	3
FOWSEQ	167.12	109.132	168.43	129.9	146.15	109.93	71.381	51.829	1.26	1.17	1	2	4	3
HAXFER	212.117	107.156	194.12	143.99	167.35	125.28	110.647	6.628	1.32	1.19	1	0	7	1
IDAHOK	167.12	79.102	167.81	104.45	145.38	88.71	72.491	6.694	1.26	1.09	1	0	4	1
IDAHUQ	167.12	105.14	166.74	138.06	144.7	120.63	71.056	6.759	1.25	1.17	1	0	4	1
IGESAQ	188.182	180.21	191.98	193.12	179.9	184.74	46.668	13.757	1.25	1.23	2	0	2	2
IGOGES	166.132	221.263	173.22	243.09	151.88	227.56	66.612	26.079	1.26	1.35	2	0	2	2
JEJNAO	212.117	156.188	192.68	178.94	166.41	164.64	109.409	13.172	1.32	1.23	1	0	7	2
KUJDIE	138.122	122.171	147.06	154.44	130.11	136.9	47.723	7.76	1.18	1.2	2	0	2	2
KUZJIZ	166.132	128.562	169.37	134.78	150.68	113.81	64.239	29.577	1.24	1.19	2	1	2	2
LOCMUM	254.15	180.21	231.16	191.77	207.2	183.76	131.338	13.887	1.37	1.23	4	0	4	2
MAHWOI	201.565	107.156	180.84	142.75	158.57	124.36	70.035	6.613	1.28	1.18	1	0	4	1
MOYSID	154.121	94.117	158.28	117.91	137.1	99.1	70.296	29.521	1.23	1.14	3	1	3	2
MOZBUA	201.019	94.117	162.56	116.47	142.32	98.44	33.714	27.061	1.23	1.13	1	1	1	2
MUGPOT	212.117	156.188	195.71	179.89	168.8	166.53	111.516	13.152	1.32	1.23	1	0	7	2
NIMDIW	138.122	145.161	147.94	161.05	130.55	147.64	48.333	26.005	1.19	1.19	2	1	2	2
OCEMUG	156.568	109.132	156.8	128.96	137.18	108.8	32.334	49.545	1.22	1.17	1	2	1	3
OGAVOJ	212.117	156.188	190.35	180.55	166.67	165.91	107.909	12.449	1.3	1.24	1	0	7	2

PEKSUV	154.121	156.188	156.61	175.99	137.42	163.93	67.321	13.857	1.22	1.21	3	0	3	2
PUFMIN	212.073	180.21	170.11	191.37	147.5	183.41	32.102	13.874	1.26	1.23	1	0	1	2
REXMUE	238.092	180.21	195.77	192.13	171.24	184.19	64.888	13.83	1.31	1.23	2	0	2	2
REXNOZ	238.092	122.171	196.1	154.4	170.92	136.81	65.567	7.69	1.32	1.2	2	0	2	2
ROFCEV	167.12	94.117	167.43	117.77	145.49	99.38	71.158	29.07	1.25	1.14	1	1	4	2
SOLHAE	152.149	122.171	172.26	154.34	151.32	136.77	42.55	7.82	1.25	1.2	1	0	2	2
SORVIG	481.716	104.112	244.65	126.36	222.83	109.09	65.904	22.106	1.38	1.14	2	0	2	2
TEKLOK	254.15	156.188	231.48	180.31	207.01	165.82	130.844	13.032	1.37	1.24	4	0	4	2
TICZOW	212.117	155.2	195.54	182.89	168.42	171.41	111.679	6.907	1.33	1.23	1	0	7	1
TIPGOQ	254.15	220.32	228.73	223.35	205.45	204.58	128.167	10.13	1.36	1.33	4	0	4	4
UNECEV	254.15	122.171	228.67	154.34	205.12	136.62	128.488	7.593	1.36	1.2	4	0	4	2
UVOKIA	303.912	108.144	228.34	135.89	205.65	117.07	64.975	28.274	1.36	1.17	2	1	2	2
UYOZEO	238.092	156.188	196.25	177.47	171.08	164.78	65.495	13.905	1.32	1.22	2	0	2	2
VIGDOF	192.258	145.165	222.57	164.1	208.43	146.99	33.952	30.937	1.31	1.22	1	1	1	3
VUKPAU	167.12	169.18	168.82	183.16	146.43	163.57	72.659	58.309	1.26	1.27	1	3	4	4
WADPAU	558.835	156.188	255.56	176.59	235.33	164.49	86.458	13.734	1.39	1.22	3	0	3	2
WAQMAD	254.15	156.188	228.96	177.51	206	164.43	128.774	13.303	1.36	1.22	4	0	4	2
XIPDAB01	167.12	145.161	166.79	161.43	144.56	147.7	71.784	26.851	1.25	1.19	1	1	4	2

Table S2: Summary of the calculated molecular properties for the acid and base molecules known to form ICCs as retrieved from the Cambridge Structural Database (CSD)[4]. The CSD refcodes listed above correspond to the ICC crystal structure. The Corey-Pauling-Koltun (CPK)[5] model was used to calculate the molecular surface area, volume, polar surface area (PSA) and molecular ovality using Spartan'16[6]. HBD=Hydrogen Bond Donor; HBA=Hydrogen Bond Acceptor. Some ICC crystal structures retrieved from the CSD were removed from the list prior to carrying out the above calculations, due to crystal disorder.

1.3 Calculated most stable polymorphs in the crystal form landscapes of Systems I-VI (using FIT potential parameter set)

Structure ID	E_{latt}/kJ mol^{-1}	Relative E_{latt}/kJ mol^{-1}	Volume /Å^3	Density /g cm^{-3}	Space Group	a / Å	b / Å	c / Å	α / °	β / °	γ / °	Kitaigorodsky Packing Index (%)
742	-617.45	0	1228.47	1.36	$P2_1/c$	6.81	20.16	9.00	90.00	96.15	90.00	68.20
722	-617.02	0.43	1181.45	1.41	$P2_1/c$	9.45	25.44	6.56	90.00	131.42	90.00	70.60
53	-616.12	1.33	590.05	1.41	P-1	13.24	9.54	6.51	48.95	83.34	97.91	70.70
786	-615.78	1.67	1286.94	1.29	$P2_1/c$	7.29	16.80	11.61	90.00	64.82	90.00	64.80
685	-614.68	2.76	1197.86	1.39	$P2_1/c$	9.51	25.37	7.23	90.00	43.41	90.00	69.80
812	-612.72	4.73	2439.02	1.37	PBCA	7.83	13.63	22.84	90.00	90.00	90.00	68.80
396	-612.49	4.96	1309.63	1.27	$P2_12_12_1$	17.22	7.26	10.47	90.00	90.00	90.00	63.80
774	-612.48	4.96	1317.64	1.26	$P2_1/c$	7.11	10.85	22.64	90.00	131.02	90.00	63.30
772	-611.68	5.77	1312.47	1.27	$P2_1/c$	11.05	16.75	12.22	90.00	144.56	90.00	63.60
694	-611.30	6.14	1323.17	1.26	$P2_1/c$	7.11	11.06	25.94	90.00	139.54	90.00	63.10
956	-610.83	6.62	2467.78	1.35	PBCA	13.74	22.99	7.81	90.00	90.00	90.00	67.90
52	-610.62	6.82	617.44	1.35	P-1	7.96	12.94	8.98	107.91	45.22	108.45	67.80
775	-610.44	7.00	1241.16	1.34	$P2_1/c$	12.34	12.53	8.03	90.00	91.97	90.00	67.40
58	-610.41	7.04	586.49	1.42	P-1	8.16	6.02	13.49	92.99	65.20	79.70	71.70
669	-610.37	7.08	1216.11	1.37	$P2_1/c$	6.72	7.19	32.61	90.00	50.53	90.00	68.60
236	-610.18	7.26	1192.45	1.40	$P2_12_12_1$	22.49	5.94	8.93	90.00	90.00	90.00	70.30
691	-609.84	7.60	1235.91	1.35	$P2_1/c$	12.33	11.85	8.47	90.00	87.61	90.00	67.80
420	-609.57	7.88	1303.41	1.28	$P2_12_12_1$	11.53	8.83	12.80	90.00	90.00	90.00	64.20
610	-609.09	8.36	589.22	1.41	$P2_1$	12.53	9.43	5.40	90.00	67.36	90.00	71.20
720	-608.65	8.79	1240.84	1.34	$P2_1/c$	13.08	12.04	8.24	90.00	73.17	90.00	67.40
693	-608.42	9.03	1248.94	1.33	$P2_1/c$	13.83	11.43	8.17	90.00	104.63	90.00	67.00
897	-608.24	9.21	2443.21	1.36	PBCA	21.73	11.56	9.73	90.00	90.00	90.00	68.50
214	-608.06	9.39	1219.68	1.37	$P2_12_12_1$	8.76	6.08	22.89	90.00	90.00	90.00	68.20
869	-608.02	9.42	2474.49	1.35	PBCA	12.13	8.07	25.27	90.00	90.00	90.00	67.70
771	-607.95	9.50	1202.51	1.38	$P2_1/c$	10.97	17.95	7.15	90.00	58.72	90.00	69.90
764	-607.89	9.56	1195.62	1.39	$P2_1/c$	11.59	9.00	11.53	90.00	95.71	90.00	70.20
852	-607.76	9.68	2526.49	1.32	PBCA	11.74	21.45	10.03	90.00	90.00	90.00	66.10
731	-607.46	9.99	1245.41	1.34	$P2_1/c$	15.03	10.05	9.60	90.00	59.14	90.00	67.10
314	-607.38	10.06	1238.33	1.34	$P2_12_12_1$	17.09	6.42	11.28	90.00	90.00	90.00	67.80

Table S3: Predicted lattice energy minima for System **I** within a relative lattice energy range of 10 kJ mol^{-1} with respect to the global minimum structure.

Structure ID	E_{latt}/kJ mol^{-1}	Relative E_{latt} / kJ mol^{-1}	Volume /Å^3	Density /g cm^{-3}	Conformation ID	Space Group	a / Å	b / Å	c / Å	α / °	β / °	γ / °	Kitaigorodsky Packing Index (%)
39	-658.76	0.00	2242.04	1.38	GM	PBCA	21.35	10.09	10.40	90.00	90.00	90.00	72.10
15	-658.38	0.38	2352.39	1.31	GM	PBCA	10.12	21.09	11.02	90.00	90.00	90.00	68.50
24	-656.85	1.91	2190.01	1.41	CONF1	PBCA	21.62	9.78	10.35	90.00	90.00	90.00	74.00
85	-656.78	1.98	2190.03	1.41	CONF7	PBCA	9.78	10.35	21.62	90.00	90.00	90.00	74.00
37	-655.06	3.69	2357.98	1.31	CONF7	PBCA	20.79	11.21	10.12	90.00	90.00	90.00	68.40
193	-654.31	4.45	560.17	1.38	CONF12	P2$_1$	5.37	10.46	10.08	90.00	81.32	90.00	72.30
44	-654.23	4.53	560.19	1.38	CONF6	P2$_1$	5.37	10.46	10.08	90.00	98.68	90.00	72.10
27	-654.15	4.61	2347.04	1.31	CONF1	PBCA	10.19	21.23	10.85	90.00	90.00	90.00	68.60
49	-654.10	4.66	2346.88	1.31	CONF7	PBCA	10.19	21.23	10.85	90.00	90.00	90.00	68.60
109	-653.63	5.12	2180.84	1.41	CONF2	PBCA	10.34	21.68	9.73	90.00	90.00	90.00	74.40
105	-653.61	5.15	2180.82	1.41	CONF8	PBCA	10.34	21.68	9.73	90.00	90.00	90.00	74.40
38	-652.41	6.35	2359.01	1.31	CONF2	PBCA	11.27	10.16	20.60	90.00	90.00	90.00	68.40
45	-652.39	6.37	2359.15	1.31	CONF8	PBCA	10.16	20.60	11.27	90.00	90.00	90.00	68.40
8	-651.82	6.94	1172.89	1.32	CONF10	P2$_1$/c	6.42	18.08	10.20	90.00	82.07	90.00	68.80
112	-651.37	7.38	2322.94	1.33	CONF1	PBCA	20.97	10.64	10.41	90.00	90.00	90.00	69.80
14	-651.28	7.47	2323.28	1.33	CONF7	PBCA	10.41	20.97	10.65	90.00	90.00	90.00	69.80
62	-651.00	7.76	2345.88	1.32	CONF2	PBCA	21.26	10.80	10.22	90.00	90.00	90.00	68.60
69	-650.97	7.79	2345.73	1.32	CONF8	PBCA	21.26	10.80	10.22	90.00	90.00	90.00	68.60
19	-649.69	9.07	1131.67	1.36	CONF6	P2$_1$/c	5.34	10.45	35.33	90.00	144.97	90.00	71.50
15	-649.40	9.35	1211.39	1.27	CONF8	P2$_1$/c	7.48	19.84	10.15	90.00	53.52	90.00	66.60
185	-649.14	9.62	558.80	1.38	CONF4	P2$_1$	10.75	10.45	5.33	90.00	68.94	90.00	72.40
112	-649.09	9.67	2175.94	1.42	CONF9	PBCA	10.34	21.74	9.68	90.00	90.00	90.00	74.70
112	-649.08	9.67	2175.89	1.42	CONF3	PBCA	21.74	9.68	10.34	90.00	90.00	90.00	74.70
39	-649.07	9.69	2359.61	1.31	CONF3	PBCA	20.35	11.34	10.22	90.00	90.00	90.00	68.50
26	-649.06	9.70	2492.86	1.24	CONF9	PBCA	9.60	14.01	18.54	90.00	90.00	90.00	64.50
26	-649.05	9.71	2492.63	1.24	CONF3	PBCA	14.01	18.53	9.60	90.00	90.00	90.00	64.50
34	-648.68	10.08	2495.93	1.24	CONF4	PBCA	13.90	18.54	9.68	90.00	90.00	90.00	64.40

Table S4: Predicted lattice energy minima for System **II** within a relative lattice energy range of 10 kJ mol^{-1} with respect to the global minimum structure.

Structure ID	E_{latt}/kJ mol^{-1}	Relative E_{latt}/kJ mol^{-1}	Volume /Å^3	Density /g cm^{-3}	Space Group	a / Å	b / Å	c / Å	α / °	β / °	γ / °	Kitaigorodsky Packing Index (%)
248	-613.64	0.00	1116.81	1.38	$P2_12_12_1$	11.05	5.40	18.72	90.00	90.00	90.00	71.80
945	-612.19	1.46	2335.99	1.32	PBCA	11.75	20.35	9.77	90.00	90.00	90.00	68.80
545	-611.93	1.72	2322.44	1.33	PBCA	11.80	11.53	17.07	90.00	90.00	90.00	69.30
956	-610.66	2.98	2202.63	1.40	PBCA	10.93	13.39	15.05	90.00	90.00	90.00	73.20
734	-610.32	3.32	2257.24	1.37	PBCA	15.82	10.66	13.38	90.00	90.00	90.00	71.30
137	-608.29	5.36	1145.24	1.35	$P2_12_12_1$	7.74	10.73	13.80	90.00	90.00	90.00	70.20
967	-608.03	5.61	2343.30	1.32	PBCA	24.27	7.80	12.38	90.00	90.00	90.00	68.70
470	-607.96	5.68	1130.27	1.36	$P2_1/c$	10.12	9.98	11.93	90.00	110.29	90.00	71.50
978	-607.74	5.90	2373.74	1.30	PBCA	13.67	9.34	18.59	90.00	90.00	90.00	67.80
534	-607.45	6.20	2264.37	1.36	PBCA	10.14	16.86	13.25	90.00	90.00	90.00	71.30
395	-606.48	7.16	590.44	1.31	$P2_1$	8.49	10.34	6.73	90.00	88.61	90.00	68.00
1000	-606.45	7.19	2336.10	1.32	PBCA	12.76	23.81	7.69	90.00	90.00	90.00	68.90
424	-605.59	8.05	584.99	1.32	$P2_1$	6.70	10.32	8.84	90.00	73.26	90.00	68.80
989	-604.92	8.72	2284.92	1.35	PBCA	16.12	12.12	11.70	90.00	90.00	90.00	70.30
387	-604.04	9.60	592.73	1.30	$P2_1$	10.59	6.04	12.63	90.00	132.79	90.00	67.60

Table S5: Predicted lattice energy minima for System **III** within a relative lattice energy range of 10 kJ mol^{-1} with respect to the global minimum structure.

Structure ID	E_{latt}/kJ mol^{-1}	Relative E_{latt}/kJ mol^{-1}	Volume /Å^3	Density /g cm^{-3}	Space Group	a / Å	b / Å	c / Å	α / °	β / °	γ / °	Kitaigorodsky Packing Index (%)
695	-582.71	0.00	1407.19	1.32	P2$_1$/c	13.93	7.91	12.80	90.00	86.25	90.00	69.80
717	-577.87	4.84	1415.03	1.31	P2$_1$/c	14.59	8.85	14.52	90.00	49.00	90.00	69.50
872	-577.34	5.37	2914.52	1.27	PBCA	12.72	27.63	8.29	90.00	90.00	90.00	67.40
62	-574.28	8.43	704.50	1.31	P-1	18.09	6.63	8.18	65.27	57.03	61.19	69.80
662	-573.78	8.93	1423.40	1.30	P2$_1$/c	16.15	7.71	11.54	90.00	97.68	90.00	69.10
923	-573.39	9.32	2836.62	1.31	PBCA	7.93	11.40	31.38	90.00	90.00	90.00	69.20
989	-573.09	9.62	2773.95	1.33	PBCA	14.60	12.01	15.82	90.00	90.00	90.00	70.90
641	-572.76	9.95	1447.47	1.28	P2$_1$/c	8.15	28.86	8.36	90.00	132.54	90.00	67.90

Table S6: Predicted lattice energy minima for System **IV** within a relative lattice energy range of 10 kJ mol^{-1} with respect to the global minimum structure.

Structure ID	E_{latt} (U_{inter}+ΔE_{intra}) /kJ mol^{-1}	Relative E_{latt} / kJ mol^{-1}	Volume /Å^3	Density /g cm^{-3}	Conformation ID	Space Group	a / Å	b / Å	c / Å	α / °	β / °	γ / °	Kitaigorodsky Packing Index

													(%)
102	-611.11	0.00	1396.13	1.24	CONF10	$P2_1/c$	9.91	15.97	12.49	90.00	44.89	90.00	68.30
97	-611.11	0.00	1396.27	1.24	CONF4	$P2_1/c$	8.88	15.98	12.49	90.00	128.04	90.00	68.30
267	-609.69	1.42	687.10	1.26	CONF0	P-1	19.80	10.95	9.64	46.10	29.86	41.80	69.40
464	-609.58	1.53	690.42	1.25	CONF0	P-1	10.14	8.09	10.01	75.43	96.79	64.22	69.00
111	-609.43	1.68	688.71	1.26	CONF9	P-1	10.95	9.82	8.16	67.67	58.47	74.00	69.30
123	-609.42	1.69	688.72	1.26	CONF3	P-1	9.65	10.11	8.16	63.99	75.40	78.74	69.40
178	-609.38	1.73	688.75	1.26	CONF8	P-1	9.67	10.94	12.59	48.35	52.31	46.18	69.30
156	-609.35	1.76	688.73	1.26	CONF2	P-1	16.46	8.17	9.67	104.86	116.92	124.30	69.30
111	-609.33	1.78	682.73	1.27	CONF5	P-1	8.08	10.01	9.55	67.70	75.84	75.70	69.90
134	-609.32	1.79	693.66	1.25	CONF5	P-1	10.25	9.97	8.05	76.08	63.51	95.69	68.80
104	-609.27	1.84	1377.00	1.26	CONF9	$P2_1/c$	8.33	14.65	12.40	90.00	65.58	90.00	69.30
134	-609.25	1.86	682.53	1.27	CONF12	P-1	8.06	11.21	9.52	80.99	103.17	59.53	69.90
145	-609.20	1.92	689.04	1.25	CONF4	P-1	8.14	10.98	10.06	81.92	64.94	58.30	69.20
123	-609.16	1.95	692.64	1.25	CONF10	P-1	8.07	17.91	9.83	112.79	111.53	124.28	68.80
111	-609.13	1.98	694.90	1.24	CONF12	P-1	8.02	10.33	9.92	95.01	76.53	63.00	68.80
145	-609.13	1.98	689.15	1.25	CONF10	P-1	8.14	15.09	9.64	82.34	75.75	37.15	69.30
111	-609.11	2.01	694.89	1.24	CONF6	P-1	8.02	10.33	9.92	95.03	76.53	63.00	68.80
11	-609.07	2.04	683.57	1.26	CONF0	P-1	8.12	9.60	10.05	66.93	104.89	105.56	69.80
104	-609.00	2.11	1380.47	1.25	CONF7	$P2_1/c$	7.89	21.46	11.66	90.00	135.67	90.00	69.10
145	-608.90	2.21	689.23	1.25	CONF1	P-1	10.20	8.17	9.69	74.91	78.83	62.55	69.20
111	-608.90	2.22	689.23	1.25	CONF7	P-1	10.20	9.69	8.17	74.94	62.57	78.87	69.30
178	-608.87	2.24	683.35	1.27	CONF10	P-1	10.02	8.11	9.57	75.06	112.57	104.65	69.80
125	-608.43	2.68	1319.36	1.31	CONF1	$P2_12_12_1$	11.08	8.75	13.61	90.00	90.00	90.00	72.40
129	-608.40	2.71	1341.86	1.29	CONF2	$P2_12_12_1$	7.73	12.30	14.11	90.00	90.00	90.00	71.20
121	-608.40	2.71	1319.40	1.31	CONF7	$P2_12_12_1$	13.61	8.75	11.08	90.00	90.00	90.00	72.40
114	-608.40	2.71	1341.81	1.29	CONF8	$P2_12_12_1$	14.11	7.73	12.30	90.00	90.00	90.00	71.20
116	-608.34	2.77	1341.56	1.29	CONF9	$P2_12_12_1$	12.27	14.06	7.78	90.00	90.00	90.00	71.20
127	-608.30	2.81	1341.67	1.29	CONF3	$P2_12_12_1$	14.05	12.27	7.78	90.00	90.00	90.00	71.20
901	-608.05	3.06	1376.50	1.26	CONF0	$P2_1/c$	8.34	14.64	12.38	90.00	114.34	90.00	69.30
139	-607.84	3.27	1317.30	1.31	CONF2	$P2_12_12_1$	11.08	8.94	13.31	90.00	90.00	90.00	72.50
124	-607.82	3.29	1317.33	1.31	CONF8	$P2_12_12_1$	8.94	13.31	11.08	90.00	90.00	90.00	72.40

114	-607.64	3.47	1343.08	1.29	CONF1	$P2_12_12_1$	12.31	7.70	14.17	90.00	90.00	90.00	71.10
99	-607.62	3.49	1343.00	1.29	CONF7	$P2_12_12_1$	7.70	14.17	12.31	90.00	90.00	90.00	71.10
118	-607.29	3.82	1342.56	1.29	CONF4	$P2_12_12_1$	12.24	7.83	14.01	90.00	90.00	90.00	71.10
160	-607.29	3.83	1342.51	1.29	CONF10	$P2_12_12_1$	12.24	14.01	7.83	90.00	90.00	90.00	71.10
543	-606.94	4.17	1347.87	1.28	CONF0	$P2_1/c$	6.91	16.08	13.26	90.00	113.76	90.00	70.70
85	-606.86	4.25	681.98	1.27	GM	$P2_1$	6.48	12.94	8.21	90.00	97.73	90.00	70.00
162	-606.67	4.44	1337.96	1.29	CONF4	$P2_12_12_1$	10.69	8.28	15.13	90.00	90.00	90.00	71.40
7	-606.66	4.45	1337.92	1.29	CONF10	$P2_12_12_1$	8.28	10.69	15.13	90.00	90.00	90.00	71.40
182	-606.59	4.52	1338.61	1.29	CONF9	$P2_12_12_1$	10.68	15.10	8.30	90.00	90.00	90.00	71.30
145	-606.58	4.53	707.75	1.22	CONF7	P-1	8.01	11.15	12.20	110.40	108.03	120.15	67.30
89	-606.58	4.54	1385.82	1.25	CONF8	$P2_1/c$	8.17	21.43	11.73	90.00	42.42	90.00	68.90
193	-606.55	4.56	1338.68	1.29	CONF3	$P2_12_12_1$	10.68	8.30	15.10	90.00	90.00	90.00	71.30
144	-606.51	4.60	1317.44	1.31	CONF3	$P2_12_12_1$	13.17	9.07	11.04	90.00	90.00	90.00	72.40
133	-606.51	4.60	1317.49	1.31	CONF9	$P2_12_12_1$	11.04	9.06	13.17	90.00	90.00	90.00	72.40
118	-606.37	4.74	1320.34	1.31	GM	$P2_12_12_1$	13.81	8.63	11.08	90.00	90.00	90.00	72.40
167	-606.35	4.76	707.94	1.22	CONF8	P-1	7.99	9.59	11.17	72.51	60.17	81.87	67.30
13	-606.19	4.92	1338.16	1.29	CONF5	$P2_12_12_1$	15.14	10.71	8.26	90.00	90.00	90.00	71.40
195	-606.18	4.93	1338.11	1.29	CONF11	$P2_12_12_1$	10.71	15.14	8.26	90.00	90.00	90.00	71.40
174	-606.09	5.02	1293.00	1.34	CONF12	$P2_12_12_1$	21.41	7.09	8.52	90.00	90.00	90.00	73.70

Table S7: Predicted lattice energy minima for System **V** within a relative lattice energy range of 5 kJ mol^{-1} with respect to the global minimum structure. Due to the dense crystal energy landscape for **V** (many predicted polymorphs within a small relative lattice energy range), only the most stable predicted structures within 5 kJ mol^{-1} are shown above.

Structure ID	**E_{latt} / kJ mol^{-1}**	**Relative E_{latt} / kJ mol^{-1}**	**Volume /Å^3**	**Density / g cm^{-3}**	**Space Group**	**a / Å**	**b / Å**	**c / Å**	**α / °**	**β / °**	**γ / °**	**Kitaigorodsky Packing Index (%)**

912	-570.51	0.00	1392.95	1.24	$P2_1/c$	13.40	8.19	12.84	90.00	98.66	90.00	68.20
978	-566.15	4.36	1353.20	1.28	$P2_1/c$	7.38	12.32	15.01	90.00	82.62	90.00	70.40
918	-565.47	5.04	1344.90	1.29	$P2_1/c$	12.06	10.50	11.76	90.00	64.55	90.00	70.50
36	-564.56	5.95	669.87	1.29	P-1	11.83	10.44	7.86	134.47	104.03	76.55	71.10
905	-564.43	6.08	1327.01	1.30	$P2_1/c$	7.10	11.62	19.14	90.00	122.79	90.00	71.80
90	-563.73	6.78	674.79	1.28	P-1	7.86	15.80	6.73	110.87	111.77	100.82	70.50
967	-563.15	7.36	1346.30	1.28	$P2_1/c$	6.90	12.52	15.72	90.00	97.31	90.00	70.80
7	-562.95	7.56	2766.05	1.25	C2/c	14.96	7.64	24.92	90.00	103.84	90.00	68.90
245	-562.82	7.69	658.92	1.31	$P2_1$	6.62	15.36	7.53	90.00	59.43	90.00	72.20
81	-562.48	8.03	695.61	1.24	P-1	12.64	7.37	8.81	60.42	77.28	82.31	68.50
276	-561.92	8.59	679.77	1.27	$P2_1$	7.16	11.77	11.04	90.00	46.91	90.00	70.00
806	-561.52	8.99	1370.68	1.26	$P2_12_12_1$	24.18	7.80	7.27	90.00	90.00	90.00	69.30
85	-561.50	9.01	688.64	1.26	P-1	6.95	19.46	7.95	83.36	114.87	133.07	69.20
51	-561.00	9.51	701.48	1.23	P-1	12.55	8.26	8.35	125.34	86.92	96.84	67.90
849	-560.80	9.72	687.32	1.26	$P2_1$	11.73	7.38	7.97	90.00	95.15	90.00	69.20
939	-560.67	9.85	1399.28	1.24	$P2_1/c$	6.76	27.76	8.06	90.00	67.75	90.00	68.00
181	-560.48	10.03	685.47	1.26	P-1	13.88	7.64	7.66	87.87	73.59	62.16	69.50

Table S8: Predicted lattice energy minima for System **VI** within a relative lattice energy range of 10 kJ mol^{-1} with respect to the global minimum structure.

1.4 DFT optimisations of the predicted most stable structures and discussion of the effect of the DFT method on the ranking of predicted structures

1.4.1 Methodology

The 20 most stable structures of systems **I** (Table S3), **III** (Table S5), **IV** (Table S6) and **VI** (Table S8) obtained following lattice energy minimisation using the empirical FIT[7-11] potential parameter set were selected for further analysis by means of periodic dispersion-corrected DFT calculations (DFT-D). Initially, all structures were optimised using the PBE functional[12] combined with the plane-wave implementation[13] of the Grimme D2 dispersion correction[14] (PBE+D2). Subsequently, the 5 lowest energy structures generated by the PBE+D2 method were re-optimised using PBE with TS dispersion correction (PBE+TS)[15] as well as uncorrected LDA functional. Periodic DFT calculations were performed using the CASTEP 16.11 code[16]. Input files were prepared with the aid of the cif2cell program[17]. Structures were geometry-optimised with respect to atom coordinates and unit cell parameters, subject to symmetry constraints of their corresponding space groups. Calculations were performed using the PBE functional[12] combined with the plane-wave implementation[13] of the Grimme D2[14] or TS[15] dispersion corrections or with uncorrected LDA functional. The plane wave basis set was truncated at 750 eV, norm-conserving OPIUM pseudopotentials[18] were used in PBE calculations, while the LDA calculations were performed with ultrasoft pseudopotentials generated by CASTEP on the fly. The following convergence criteria for geometry optimisation were used: maximum energy change between iterations 10^{-5} eV/atom, maximum force on atom 0.03 eV/Å, maximum atom displacement 0.001 Å and residual stress 0.05 GPa. The 1st Brillouin zone was sampled with 0.03 $Å^{-1}$ Monkhorst-Pack *k*-point grid[19].

The purpose of these calculations was to compare the empirical FIT[7-11] energy ranking with the periodic DFT approach, as well as to investigate the differences between crystal form landscapes produced by different DFT methods. Due to the computational cost of these DFT optimisations, the results (see Tables S9-S12) are limited to systems **I**, **III**, **IV** and **VI**. The Grimme D2 dispersion correction is based on a parameterised set of C_6 dispersion coefficients for a number of elements. The dispersion energy is then computed as a sum of pairwise atom-atom interactions. In the TS scheme the C_6 coefficients are computed from the electron density of the crystal structure, therefore the TS approach may be considered more system-specific. Finally, LDA functional is known to produce stronger supramolecular forces compared to GGA counterparts. It is for that reason that LDA functional may produce energy rankings comparable to dispersion-corrected GGA functionals. Recently a comparison of dispersion-corrected PBE and LDA was reported for MOF-type materials based on pentazolate ligands[20]. For these systems LDA energy ranking was found to follow dispersion-corrected PBE. It was therefore considered interesting to perform a similar study for the structures of organic salts. The results of periodic DFT calculations are summarised in Tables S9-S12 and are discussed in section 1.4.3.

1.4.2 Structural parameters and relative lattice energy of the DFT-D optimised structures for Systems I, III, IV and VI

1.4.2.1 System I

Structure ID*	Relative E_{latt} (PBE+D2)/ kJ mol^{-1}	Volume / Å^3	Z	a / Å	b / Å	c / Å	α / °	β / °	γ / °
I_RANK-10_694	0.00	1298.80	4	7.30	11.40	25.85	90.00	142.84	90.00
I_RANK-8_774	0.26	1286.37	4	7.14	10.82	23.27	90.00	134.33	90.00
I_RANK-9_772	0.49	1274.97	4	11.10	16.17	11.98	90.00	143.64	90.00
I_RANK-18_420	0.78	1273.56	4	11.87	8.33	12.88	90.00	90.00	90.00
I_RANK-7_396	2.34	1284.88	4	16.05	7.40	10.82	90.00	90.00	90.00
I_RANK-4_786	2.49	1285.70	4	7.23	16.46	12.03	90.00	63.82	90.00
I_RANK-16_236	3.17	1155.46	4	22.66	5.61	9.09	90.00	90.00	90.00
I_RANK-20_720	3.56	1187.61	4	13.44	11.55	8.04	90.00	72.02	90.00
I_RANK-12_52	5.60	589.08	2	7.74	12.94	8.82	107.92	46.38	112.64
I_RANK-2_722	5.76	1124.18	4	9.29	25.81	6.37	90.00	132.60	90.00
I_RANK-13_775	5.87	1197.15	4	12.40	12.20	7.93	90.00	86.70	90.00
I_RANK-19_610	6.24	579.12	2	12.14	9.49	5.37	90.00	69.33	90.00
I_RANK-6_812	7.41	2378.01	8	7.64	13.34	23.35	90.00	90.00	90.00
I_RANK-17_691	7.58	1216.15	4	12.55	11.59	8.36	90.00	89.49	90.00
I_RANK-14_58	8.15	570.00	2	8.23	5.78	13.47	94.59	67.51	77.88
I_RANK-3_53	8.17	570.10	2	13.60	9.25	6.27	49.80	85.34	100.86
I_RANK-1_742	8.66	1203.99	4	6.63	20.61	8.91	90.00	98.74	90.00
I_RANK-11_956	10.55	2388.39	8	13.34	23.72	7.55	90.00	90.00	90.00
I_RANK-5_685	12.21	1165.25	4	9.24	25.98	7.10	90.00	43.15	90.00
I_RANK-15_669	13.56	1157.97	4	6.44	7.04	31.46	90.00	54.31	90.00

Structure ID*	Relative E_{latt} (PBE+TS)/ kJ mol^{-1}	Volume / Å^3	Z	a / Å	b / Å	c / Å	α / °	β / °	γ / °
I_RANK-10_694	0.00	1319.08	4	7.19	11.47	25.59	90.00	141.31	90.00
I_RANK-9_772	0.31	1303.34	4	11.06	16.63	12.01	90.00	143.84	90.00
I_RANK-8_774	2.09	1320.72	4	7.13	10.62	23.74	90.00	132.73	90.00

I_RANK-7_396	2.21	1319.71	4	16.63	7.36	10.78	90.00	90.00	90.00
I_RANK-18_420	2.94	1310.33	4	11.99	8.54	12.79	90.00	90.00	90.00

Structure ID*	Relative E_{latt} (LDA)/ kJ mol^{-1}	Volume / Å^3	Z	a / Å	b / Å	c / Å	α / °	β / °	γ / °
I_RANK-8_774	0.00	1201.51	4	7.02	10.57	22.88	90.00	134.91	90.00
I_RANK-7_396	0.92	1190.45	4	15.72	7.28	10.40	90.00	90.00	90.00
I_RANK-10_694	1.11	1209.13	4	7.10	11.24	25.05	90.00	142.75	90.00
I_RANK-9_772	1.47	1187.00	4	10.78	15.82	11.68	90.00	143.43	90.00
I_RANK-18_420	3.91	1184.02	4	11.66	8.18	12.41	90.00	90.00	90.00

Table S9: Calculated lattice parameters and relative lattice energies of the DFT optimised structures for System **I** as a function of the DFT method used. The 5 most stable structures obtained following PBE+D2 optimisations of the predicted crystal structures of **I** (from a pool of the most stable 20 structures of this system that were predicted using the FIT empirical force field) were used to test the effect of changing the energy model on the ranking of the predicted structure on the crystal form landscape. This was done by re-optimising these 5 most stable structures after PBE+D2 optimisation using either the PBE+TS or LDA methods. The above entries summarize the results of these DFT optimisations. The relative energy and all other lattice parameters listed above are those calculated following CASTEP geometry optimisation of the predicted structure at the appropriate level of theory. * In the structure ID column, the rank mentioned refers to that found following crystal structure prediction using the empirical FIT potential parameters.

1.4.2.2 System III

Structure ID*	Relative E_{latt} (PBE+D2)/ kJ mol^{-1}	Volume / Å^3	Z	a / Å	b / Å	c / Å	α / °	β / °	γ / °
III_RANK-3_545	0.00	2229.32	8	12.43	11.26	15.93	90.00	90.00	90.00
III_RANK-1_248	1.89	1069.90	4	11.08	5.60	17.22	90.00	90.00	90.00
III_RANK-2_945	3.53	2262.13	8	11.66	19.25	10.08	90.00	90.00	90.00
III_RANK-8_470	4.85	1098.79	4	10.54	9.30	11.79	90.00	108.04	90.00
III_RANK-9_978	6.05	2243.90	8	13.78	8.34	19.52	90.00	90.00	90.00
III_RANK-4_956	6.20	2178.14	8	11.00	13.61	14.55	90.00	90.00	90.00
III_RANK-6_137	7.70	1100.39	4	7.23	11.08	13.74	90.00	90.00	90.00
III_RANK-5_734	9.66	2222.40	8	15.41	10.78	13.38	90.00	90.00	90.00
III_RANK-14_989	9.70	2223.79	8	15.02	12.11	12.23	90.00	90.00	90.00
III_RANK-10_534	12.74	2195.34	8	10.41	15.76	13.38	90.00	90.00	90.00
III_RANK-20_15	13.24	551.71	2	9.23	5.56	12.49	90.00	59.33	90.00
III_RANK-13_424	13.69	564.24	2	6.70	10.51	8.74	90.00	66.50	90.00
III_RANK-15_387	13.82	568.80	2	10.55	6.34	12.70	90.00	137.97	90.00
III_RANK-11_395	15.75	572.83	2	8.19	10.47	6.72	90.00	83.38	90.00
III_RANK-17_678	17.20	2265.57	8	12.05	21.60	8.70	90.00	90.00	90.00
III_RANK-7_967	17.23	2243.60	8	23.88	7.60	12.36	90.00	90.00	90.00
III_RANK-12_1000	20.17	2281.79	8	12.68	23.49	7.66	90.00	90.00	90.00
III_RANK-16_103	20.50	1178.95	4	18.11	5.91	11.01	90.00	90.00	90.00
III_RANK-19_845	21.88	2331.92	8	20.45	9.40	12.13	90.00	90.00	90.00
III_RANK-18_645	23.68	2374.04	8	12.44	9.33	20.44	90.00	90.00	90.00

Structure ID*	Relative E_{latt} (PBE+TS)/ kJ mol^{-1}	Volume / Å^3	Z	a / Å	b / Å	c / Å	α / °	β / °	γ / °
III_RANK-1_248	0.00	1093.95	4	11.12	5.53	17.79	90.00	90.00	90.00
III_RANK-3_545	4.59	2282.04	8	12.29	11.34	16.37	90.00	90.00	90.00
III_RANK-8_470	5.61	1133.01	4	10.70	9.45	11.94	90.00	110.24	90.00

III_RANK-2_945	8.12	2312.89	8	11.73	19.53	10.09	90.00	90.00	90.00
III_RANK-9_978	10.99	2326.85	8	13.80	8.63	19.54	90.00	90.00	90.00

Structure ID*	**Relative E_{latt} (LDA)/ kJ mol^{-1}**	**Volume / Å^3**	**Z**	**a / Å**	**b / Å**	**c / Å**	**α / °**	**β / °**	**γ / °**
III_RANK-1_248	0.00	1006.87	4	10.91	5.50	16.79	90.00	90.00	90.00
III_RANK-3_545	6.02	2062.20	8	12.59	11.01	14.87	90.00	90.00	90.00
III_RANK-2_945	8.46	2131.38	8	11.45	18.74	9.93	90.00	90.00	90.00
III_RANK-9_978	9.88	2102.32	8	13.38	8.06	19.49	90.00	90.00	90.00
III_RANK-8_470	11.07	1019.01	4	9.88	9.46	11.57	90.00	109.52	90.00

Table S10: Calculated lattice parameters and relative lattice energies of the DFT optimised structures for System **III** as a function of the DFT method used. The 5 most stable structures obtained following PBE+D2 optimisations of the predicted crystal structures of **III** (from a pool of the most stable 20 structures of this system that were predicted using the FIT empirical force field) were used to test the effect of changing the energy model on the ranking of the predicted structure on the crystal form landscape. This was done by re-optimising these 5 most stable structures after PBE+D2 optimisation using either the PBE+TS or LDA methods. The above entries summarize the results of these DFT optimisations. The relative energy and all other lattice parameters listed above are those calculated following CASTEP geometry optimisation of the predicted structure at the appropriate level of theory. * In the structure ID column, the rank mentioned refers to that found following crystal structure prediction using the empirical FIT potential parameters.

1.4.2.3 System IV

Structure ID*	**Relative E_{latt} (PBE+D2)/ kJ mol^{-1}**	**Volume / Å^3**	**Z**	**a / Å**	**b / Å**	**c / Å**	**α / °**	**β / °**	**γ / °**
IV_RANK-17_334	0.00	1319.52	4	12.12	8.94	12.17	90.00	90.00	90.00

IV_RANK-7_989	2.32	2576.75	8	13.94	11.76	15.72	90.00	90.00	90.00
IV_RANK-1_695	3.17	1301.20	4	14.00	7.67	12.13	90.00	86.96	90.00
IV_RANK-5_662	4.12	1302.03	4	16.37	7.33	10.91	90.00	96.11	90.00
IV_RANK-6_923	4.90	2586.11	8	7.48	11.02	31.35	90.00	90.00	90.00
IV_RANK-2_717	5.09	1297.18	4	14.35	8.16	14.54	90.00	49.63	90.00
IV_RANK-11_729	5.23	1301.13	4	7.13	20.89	10.68	90.00	54.90	90.00
IV_RANK-19_726	5.83	1321.43	4	8.85	14.31	18.48	90.00	145.60	90.00
IV_RANK-8_641	6.13	1310.09	4	7.88	29.47	7.81	90.00	133.73	90.00
IV_RANK-3_872	6.37	2692.37	8	12.20	27.87	7.92	90.00	90.00	90.00
IV_RANK-4_62	7.67	646.53	2	17.99	6.18	7.70	67.82	59.05	63.88
IV_RANK-10_35	8.05	650.30	2	6.07	8.35	16.90	126.16	105.94	70.94
IV_RANK-20_739	8.22	1363.89	4	9.51	18.84	7.76	90.00	101.28	90.00
IV_RANK-9_19	8.79	661.72	2	15.57	6.77	7.11	114.62	77.61	100.69
IV_RANK-16_18	8.90	645.39	2	15.58	6.20	6.98	76.38	85.25	80.30
IV_RANK-13_691	10.05	1323.52	4	7.68	30.31	7.97	90.00	45.50	90.00
IV_RANK-14_17	10.83	650.61	2	6.83	15.42	7.19	104.30	116.91	78.08
IV_RANK-15_16	11.41	642.35	2	6.65	7.13	14.42	84.04	94.33	71.72
IV_RANK-12_934	13.69	2673.87	8	32.76	8.53	9.56	90.00	90.00	90.00
IV_RANK-18_723	17.28	1298.08	4	12.26	13.97	9.18	90.00	55.65	90.00

Structure ID*	**Relative E_{latt} (PBE+TS)/ kJ mol^{-1}**	**Volume / Å^3**	**Z**	**a / Å**	**b / Å**	**c / Å**	**α / °**	**β / °**	**γ / °**
IV_RANK-7_989	0.00	2652.82	8	14.44	11.73	15.66	90.00	90.00	90.00

IV_RANK-17_334	1.70	1364.38	4	12.40	8.95	12.30	90.00	90.00	90.00
IV_RANK-1_695	2.60	1348.44	4	13.86	7.97	12.22	90.00	87.87	90.00
IV_RANK-6_923	3.07	2658.91	8	7.65	11.11	31.28	90.00	90.00	90.00
IV_RANK-5_662	5.96	1349.58	4	16.34	7.54	11.02	90.00	96.54	90.00

Structure ID*	**Relative E_{latt} (LDA)/ kJ mol^{-1}**	**Volume / Å^3**	**Z**	**a / Å**	**b / Å**	**c / Å**	**α / °**	**β / °**	**γ / °**
IV_RANK-17_334	0.00	1229.92	4	11.80	8.76	11.89	90.00	90.00	90.00
IV_RANK-7_989	6.49	2395.69	8	13.77	11.39	15.26	90.00	90.00	90.00
IV_RANK-1_695	8.97	1209.03	4	13.54	7.55	11.83	90.00	87.98	90.00
IV_RANK-6_923	10.50	2401.93	8	7.28	10.69	30.85	90.00	90.00	90.00
IV_RANK-5_662	11.02	1212.78	4	16.07	7.16	10.61	90.00	96.62	90.00

Table S11: Calculated lattice parameters and relative lattice energies of the DFT optimised structures for System **IV** as a function of the DFT method used. The 5 most stable structures obtained following PBE+D2 optimisations of the predicted crystal structures of **IV** (from a pool of the most stable 20 structures of this system that were predicted using the FIT empirical force field) were used to test the effect of changing the energy model on the ranking of the predicted structure on the crystal form landscape. This was done by re-optimising these 5 most stable structures after PBE+D2 optimisation using either the PBE+TS or LDA methods. The above entries summarize the results of these DFT optimisations. The relative energy and all other lattice parameters listed above are those calculated following CASTEP geometry optimisation of the predicted structure at the appropriate level of theory. * In the structure ID column, the rank mentioned refers to that found following crystal structure prediction using the empirical FIT potential parameters.

1.4.2.4 System VI

Structure ID*	**Relative E_{latt} (PBE+D2)/ kJ**	**Volume / Å^3**	**Z**	**a / Å**	**b / Å**	**c / Å**	**α / °**	**β / °**	**γ / °**

	mol^{-1}								
VI_RANK-3_918	0.00	1224.42	4	11.70	10.47	11.42	90.00	61.07	90.00
VI_RANK-5_905	0.89	1213.13	4	6.85	11.12	18.81	90.00	122.16	90.00
VI_RANK-12_806	3.21	1257.42	4	23.92	7.38	7.12	90.00	90.00	90.00
VI_RANK-1_912	3.61	1299.26	4	13.53	7.80	12.50	90.00	100.15	90.00
VI_RANK-15_849	4.20	646.42	2	11.28	7.38	7.80	90.00	95.75	90.00
VI_RANK-10_81	4.75	625.54	2	12.60	6.82	8.31	64.16	77.52	88.56
VI_RANK-14_51	5.79	632.80	2	12.00	7.80	8.18	123.62	84.87	96.83
VI_RANK-4_36	6.82	634.58	2	11.90	10.94	7.16	134.36	103.52	72.36
VI_RANK-9_245	7.05	623.96	2	6.46	15.25	7.29	90.00	60.28	90.00
VI_RANK-13_85	7.13	627.19	2	6.68	19.02	7.89	83.94	115.89	133.30
VI_RANK-11_276	7.66	624.70	2	6.96	11.41	11.01	90.00	45.66	90.00
VI_RANK-2_978	8.05	1277.89	4	7.18	12.01	14.96	90.00	82.67	90.00
VI_RANK-20_920	8.30	1282.25	4	7.70	22.42	7.42	90.00	90.25	90.00
VI_RANK-19_970	8.67	1263.75	4	8.26	23.32	7.31	90.00	63.85	90.00
VI_RANK-17_181	9.32	637.43	2	13.88	7.47	7.56	88.26	72.12	59.92
VI_RANK-6_90	9.92	629.04	2	7.60	15.50	6.59	110.24	111.42	101.64
VI_RANK-18_37	11.66	630.48	2	13.05	7.66	7.10	85.98	63.93	95.30
VI_RANK-8_7	11.73	1283.12	4	7.84	7.84	25.44	98.51	98.51	56.35
VI_RANK-7_967	12.10	1253.78	4	6.71	12.17	15.51	90.00	97.93	90.00
VI_RANK-16_939	13.24	1309.89	4	6.61	27.66	7.70	90.00	68.47	90.00

Structure ID*	**Relative E_{latt} (PBE+TS)/ kJ mol^{-1}**	**Volume / Å^3**	**Z**	**a / Å**	**b / Å**	**c / Å**	**α / °**	**β / °**	**γ / °**
VI_RANK-5_905	0.00	1262.83	4	7.09	11.30	18.84	90.00	123.26	90.00
VI_RANK-15_849	1.14	645.34	2	11.43	7.22	7.87	90.00	96.72	90.00

VI_RANK-3_918	2.00	1283.13	4	11.83	10.60	11.63	90.00	61.71	90.00
VI_RANK-1_912	2.26	1321.89	4	13.51	7.97	12.45	90.00	99.60	90.00
VI_RANK-12_806	2.32	1299.82	4	23.89	7.63	7.13	90.00	90.00	90.00

Structure ID*	**Relative E_{latt} (LDA)/ kJ mol^{-1}**	**Volume / Å^3**	**Z**	**a / Å**	**b / Å**	**c / Å**	**α / °**	**β / °**	**γ / °**
VI_RANK-1_912	0.00	1176.82	4	14.28	7.10	11.77	90.00	99.58	90.00
VI_RANK-5_905	9.56	1125.59	4	6.78	10.70	17.72	90.00	118.96	90.00
VI_RANK-15_849	10.87	596.36	2	10.80	7.05	7.90	90.00	97.90	90.00
VI_RANK-3_918	11.09	1148.86	4	11.57	10.14	11.20	90.00	61.01	90.00
VI_RANK-12_806	11.35	1168.68	4	23.21	7.26	6.94	90.00	90.00	90.00

Table S12: Calculated lattice parameters and relative lattice energies of the DFT optimised structures for System **VI** as a function of the DFT method used. The 5 most stable structures obtained following PBE+D2 optimisations of the predicted crystal structures of **VI** (from a pool of the most stable 20 structures of this system that were predicted using the FIT empirical force field) were used to test the effect of changing the energy model on the ranking of the predicted structure on the crystal form landscape. This was done by re-optimising these 5 most stable structures after PBE+D2 optimisation using either the PBE+TS or LDA methods. The above entries summarize the results of these DFT optimisations. The relative energy and all other lattice parameters listed above are those calculated following CASTEP geometry optimisation of the predicted structure at the appropriate level of theory. * In the structure ID column, the rank mentioned refers to that found following crystal structure prediction using the empirical FIT potential parameters.

1.4.3 Comparison of the rankings of predicted structures using the FIT potential parameters and DFT-D methods

The predicted structures (up to rank 20) for **I, III, IV** and **VI** (see Table 1 in the manuscript for more details about these salt systems) obtained following lattice energy minimisation using the empirical FIT (with multipole electrostatic model) potential parameter set were used as starting points for PBE+D2 structural optimisations (see section 1.4.1 above for more details) in order to assess the sensitivity of the structural rankings to the energy model used. Subsequent optimisations were performed using the PBE+TS and LDA methods. The starting point for these subsequent DFT optimisations were the most stable 5 structures for each of the above systems as calculated using the PBE+D2 method (see section 1.4.1 for more details). System **I** does not have any reported salt or ionic cocrystal structures in the CSD whilst for **IV**, the search for hypothetical crystal structures did not find the known salt structure amongst the set of putative crystal packings generated from the Polymorph Predictor search. For both systems, we find significant differences in the rankings of the hypothetical salt polymorphs (see Table S9 and Table S11) when the relative lattice energies from the DMACRYS calculations using the empirical FIT potential parameters are compared with the results of DFT optimisations. This is generally the case irrespective of the dispersion correction scheme used. For **III** (see Table S10)**,** the experimental structure changes from rank 3 (empirical FIT potential) to rank 1 (PBE+D2). When the PBE+TS and LDA methods are used to carry out the DFT optimisation, the experimental structure becomes the second ranked polymorph with a relative energy of 4.59 kJ mol^{-1} (PBE+TS) and 6.02 kJ mol^{-1} (LDA) with respect to the global minimum structure. The top ranked 3 structures obtained using the empirical force field remain the most stable 3 structures with the PBE+D2 and LDA methods. However, a look at the extended list of rankings following PBE+D2 optimisations of the most stable 20 structures obtained following DMACRYS lattice energy minimisation using the FIT force field, shows that there are significant re-rankings in the predicted polymorphs of **III**. This is indicated by the observation that the 8th and 9th ranked structures following DMACRYS optimisation are now observed to be the rank 4 and 5 structures respectively following PBE+D2 optimisations. By contrast for **VI** (see Table S12), the experimental global minimum structure changes from rank 1 (empirical FIT potential) to rank 4 using both the PBE+D2 and PBE+TS methods with estimated relative energies of 3.61 kJ mol^{-1} and 2.26 kJ mol^{-1} respectively with respect to the global minimum structure calculated using these respective DFT methods. Using the LDA approach however, the experimental structure is calculated to be the global minimum structure. It is noteworthy that the energy difference between the experimental global minimum structure and the next most stable structure is approximately 9.56 kJ mol^{-1} using the LDA method, which is significantly higher than seen with either the empirical force field or with the PBE+D2 and PBE+TS methods. For both **III** and **VI**, the calculated global minimum structures following PBE+D2 optimisations display sensible hydrogen bond heterosynthons (see below) between the ions that are the same as those observed in the experimental crystal structures of **III** (**DUSYOG**[21]) and **VI** (**KUJDEA**[22]). It is therefore conceivable that the re-rankings observed following PBE+D2 optimisations for **VI** point towards the existence of other polymorphs of this salt that are yet to be crystallised in the laboratory. This is possible since single crystals of 4-dimethylaminopyridinium 2-hydroxybenzoate (**KUJDEA**) were reportedly[22] crystallised following solvent evaporation of a methanol solution of equimolar amounts of 4-dimethylaminopyridine and 2-hydroxybenzoic acid. No extensive polymorph screen for other crystal forms of this salt were performed.

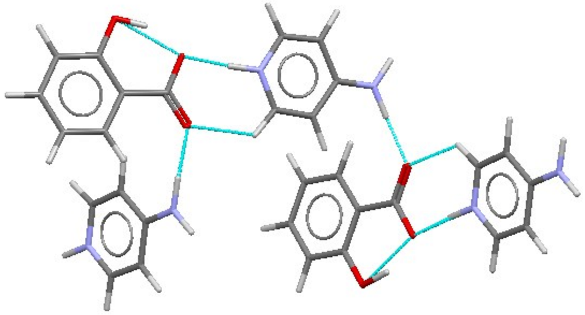

III_RANK-3_545

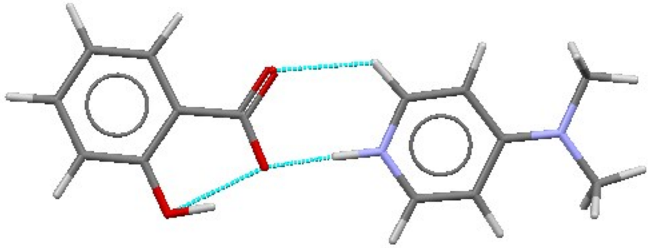

VI_RANK-3_918

Bibliography:

1. A. Mukherjee and G. R. Desiraju, *Crystal Growth & Design*, 2014, **14**, 1375-1385.
2. H. P. G. Thompson and G. M. Day, *Chemical Science*, 2014, **5**, 3173-3182.

3. M. J. Frisch, G. W. Trucks, H. B. Schlegel, G. E. Scuseria, M. A. Robb, J. R. Cheeseman, G. Scalmani, V. Barone, B. Mennucci, G. A. Petersson, H. Nakatsuji, M. Caricato, X. Li, H. P. Hratchian, A. F. Izmaylov, J. Bloino, G. Zheng, J. L. Sonnenberg, M. Hada, M. Ehara, K. Toyota, R. Fukuda, J. Hasegawa, M. Ishida, T. Nakajima, Y. Honda, O. Kitao, H. Nakai, T. Vreven, J. A. Montgomery Jr., J. E. Peralta, F. Ogliaro, M. J. Bearpark, J. Heyd, E. N. Brothers, K. N. Kudin, V. N. Staroverov, R. Kobayashi, J. Normand, K. Raghavachari, A. P. Rendell, J. C. Burant, S. S. Iyengar, J. Tomasi, M. Cossi, N. Rega, N. J. Millam, M. Klene, J. E. Knox, J. B. Cross, V. Bakken, C. Adamo, J. Jaramillo, R. Gomperts, R. E. Stratmann, O. Yazyev, A. J. Austin, R. Cammi, C. Pomelli, J. W. Ochterski, R. L. Martin, K. Morokuma, V. G. Zakrzewski, G. A. Voth, P. Salvador, J. J. Dannenberg, S. Dapprich, A. D. Daniels, Ö. Farkas, J. B. Foresman, J. V. Ortiz, J. Cioslowski and D. J. Fox, *Gaussian 09* Revision D.01, Wallingford, CT, USA, 2009.
4. C. R. Groom, I. J. Bruno, M. P. Lightfoot and S. C. Ward, *Acta Crystallographica Section B*, 2016, **72**, 171-179.
5. W. L. Koltun, *Biopolymers*, 1965, **3**, 665-679.
6. Wavefunction Inc. , *Spartan'16*, Version 2.0.7, 18401 Von Karman Ave., Suite 370, Irvine CA 92612, 2017.
7. L.-Y. Hsu and D. E. Williams, *Acta Crystallographica Section A*, 1980, **36**, 277-281.
8. S. R. Cox, L.-Y. Hsu and D. E. Williams, *Acta Crystallographica Section A*, 1981, **37**, 293-301.
9. D. E. Williams and S. R. Cox, *Acta Crystallographica Section B*, 1984, **40**, 404-417.
10. D. S. Coombes, S. L. Price, D. J. Willock and M. Leslie, *The Journal of Physical Chemistry*, 1996, **100**, 7352-7360.
11. T. Beyer and S. L. Price, *The Journal of Physical Chemistry B*, 2000, **104**, 2647-2655.
12. J. P. Perdew, K. Burke and M. Ernzerhof, *Phys. Rev. Lett.*, 1996, **77**, 3865-3868.
13. E. R. McNellis, J. Meyer and K. Reuter, *Physical Review B*, 2009, **80**, 205414.
14. S. Grimme, *Journal of Computational Chemistry*, 2006, **27**, 1787-1799.
15. A. Tkatchenko and M. Scheffler, *Phys. Rev. Lett.*, 2009, **102**, 073005.
16. S. J. Clark, M. D. Segall, C. J. Pickard, P. J. Hasnip, M. J. Probert, K. Refson and M. C. Payne, *Z. Kristall.*, 2005, **220**, 567-570.
17. T. Björkman, *Computer Physics Communications*, 2011, **182**, 1183-1186.
18. N. J. Ramer and A. M. Rappe, *Physical Review B*, 1999, **59**, 12471-12478.
19. H. J. Monkhorst and J. D. Pack, *Physical Review B*, 1976, **13**, 5188-5192.
20. M. Arhangelskis, A. D. Katsenis, A. J. Morris and T. Friscic, *Chemical Science*, 2018, DOI: 10.1039/C7SC05020H.
21. H.-K. Fun, M. Hemamalini and V. Rajakannan, *Acta Crystallographica Section E*, 2010, **66**, o2010-o2011.
22. B. Lou, S. R. Perumalla and C. C. Sun, *Crystal Growth & Design*, 2015, **15**, 24-28.